Biocatalysis and Agricultural Biotechnology 20 (2019) 101257

Contents lists available at ScienceDirect

Biocatalysis and Agricultural Biotechnology

journal homepage: www.elsevier.com/locate/bab

Characterization, antimicrobial, and antioxidant activities of silver nanoparticles synthesized by uricase from *Alcaligenes faecalis* GH3

Arastoo Badoei-dalfard*, Mojtaba Shaban, Zahra Karami

Department of Biology, Faculty of Sciences, Shahid Bahonar University of Kerman, Kerman, Iran

ARTICLE INFO

Keywords:
Uricase
Silver nanoparticles
Antibacterial
Antioxidant
Characterization

ABSTRACT

Enzyme-mediated nanoparticles synthesis has found promising attention by researchers. In this project, a powerful uricase-producing bacterium was screened from poultry soil samples which are generally rich in uric acid. GH3 isolate was identified as *Alcaligenes -faecalis*. Biosynthesis of AgNPs was done using the cell extract of *A. faecalis* GH3 treated with an aqueous solution of $AgNO_3$. SEM results show that AgNPs were spherical in shape and were in size ranging from 32 to 49 nm. Also, the zeta potential of synthesized AgNPs in colloidal solution was −21 mV, which displays the good stability of the particles in the colloidal solution. Results showed that the maximum improvement in antibacterial activity of AgNPs mixed with antibiotic was about 162.5% for ampicillin against *B. cereus*, compared to antibiotic alone. Furthermore DPPH and $ABTS^+$ radical scavenging activities showed increased activities with increasing concentration of AgNPs. IC_{50} values of AgNPs was obtained as 710 and 220 μg/ml for DPPH and $ABTS^+$ scavenging activities, respectively. These results indicate that AgNPs synthesis by cell extract of uricase producing *Alcaligenes* has potent application in antibacterial and antioxidant approaches.

1. Introduction

Nowadays silver nanoparticles are one of the greatest commercialized nanoparticles having a lot of applications in catalysis, molecular diagnostics, textile, cosmetics, photography, and photonics (Singh et al., 2015; Fariq et al., 2017). In addition, AgNPs have been used as antimicrobial mediators in surgical bandages, dental hygiene, bone substitute biomaterials, and eye treatment (Sharma et al., 2015; Fariq et al., 2017). Conventional chemical and physical methods of synthesis of nanoparticles are related to high energy consumption, and the contribution of toxic compounds which make them not to be environmental friendly. Moreover, researchers have cautioned the probable risks of exposure to AgNPs produced using diverse chemical procedures (Nakkala et al., 2017). Some recent papers have shown the toxic outcome of orally ordered PVP-coated AgNPs and sulfadiazine AgNPs, which gathered in kidney and liver and caused toxicity (Chaby et al., 2005; Van der zande et al., 2012). In recent years, green chemistry methods have encouraged scientists to synthesis nanoparticles by consuming green approaches (Shivaji et al., 2011; Rajeshkumar et al., 2016; Fariq et al., 2017; Premkumar et al., 2018; Nanda et al., 2018; Vijayabharathi et al., 2018).

Because of using nontoxic, eco-friendly compounds, and moderately easier production procedure at ambient environments in green creation of AgNPs, it has gained remarkable impact against physical and chemical techniques (Singh et al., 2013; Ghosh, and Sarkar, 2014; Ocsoy et al., 2018). Furthermore, biomolecules act as a stabilizing agent for AgNPs, which preventing from the time-course of aggregation of AgNPs more than chemical methods (Singh et al., 2013; Ocsoy et al., 2018). Due to easy cultivation, fast growth rate, and capability to develop at ambient environments of temperature, pressure, and pH of bacteria species, they are generally preferred for nanoparticles (NPs) synthesis. Some bacteria like *Bacillus* (Wei et al., 2012; Priyadarshinia et al., 2013; Velmurugan et al., 2014; Lateef et al., 2016a,b; Ghiut et al., 2018), *Stenotrophomonas maltophilia* MKH1(Rostami et al., 2018), *Streptomyces* (Abd-Elnaby et al., 2016), *Escherichia coli* (Viswanathan et al., 2016), and *Lysinibacillus* (Bhatia et al., 2016) have been employed for green synthesis of nanoparticles.

Bacterial production of nanoparticles occurs either intra- or extracellularly concerning the localization of the reductive elements (Fariq et al., 2017). Intracellular process of NPs production involves supplementary phases to isolate the gathered nanoparticles from bacterial cells and, consequently is less favored (Sneha, and Yun, 2013; Kalishwaralal et al., 2010; Singh et al., 2015). Some new approach for extracellular NP synthesis is synthesis using cell-free extract (CFE) and culture supernatant (Kumar and Mamidyala, 2011; Shivaji et al., 2011; Zonooz and Salouti, 2011). In the first strategy, silver nanoparticles

* Corresponding author.
E-mail address: badoei@uk.ac.ir (A. Badoei-dalfard).

https://doi.org/10.1016/j.bcab.2019.101257
Received 10 June 2019; Received in revised form 18 July 2019; Accepted 18 July 2019
Available online 19 July 2019
1878-8181/

produced from culture supernatant surround in the media constituents, which could impede their colloidal dispersion, retrieval, and characterization (Singh et al., 2015). Although, the last method confirms the complete elimination of organic media constituents and bacterial biomass (Singh et al., 2013, 2015), but long period of incubation of bacteria in distilled water may be inactivate biomolecules, especially enzymes.

In an efficient approach for NPs synthesis, well-grown bacteria could be washed, centrifuged, and then sonicated in ice. Cell free extract was used a high concentrated and an ideal source for organic molecules and biomolecules, especially reductive enzymes (Wei et al., 2012; Gholami-Shabani et al., 2015; Wadhwani et al., 2018). This technique not only confirms the whole elimination of organic media components and bacterial biomass through frequent washings, but also protects biomolecules against denaturation and proteolytic degradation. It qualifies nanoparticles to be produced just from organic biomolecules produced.

Up to now, several enzymes such as alpha amylase, laccase, keratinase, xylanase, nitrate reductase, and protease have been used for synthesis of AgNPs (Lateef et al., 2015a,b; Lateef et al., 2015a,b; Adelere and Lateef, 2016; Elegbede et al., 2018a,b). These nanoparticles showed excellent properties, such as antioxidant, larvicidal, anticoagulant and thrombolytic activities. The process may also be catalyzed by whole enzyme or amino acids released due to enzyme denaturation during reaction processes. Durán et al. (2014) showed the participation of thiol groups and disulfide bounds of enzymes as the reaction sites of nanoparticles synthesis. Similarly, the S–S and S–H bounds of denatured enzymes could convert metallic ions to nanoparticles (Durán et al., 2014; Adelere and Lateef, 2016).

In the current study, cell extract of *Alcaligenes faecalis* GH3 was applied in green synthesis of AgNPs. This isolate which screened from soil produced a high potent uricase as a reductive enzyme. Effects of different factors such as time, Ag concentration, pH and temperature on the creation of AgNPs was also optimized. The created Ag nanoparticles were characterized by analytical techniques. Their antimicrobial activities were evaluated against the pathogenic Gram-positive and Gram-negative bacteria, and the antioxidant activities also determined.

2. Materials and methods

2.1. Screening of uricase-producing bacteria

Since birds are uricotelic animals, poultry soils samples are generally deliberated to be rich in uric acid. These soils were gathered from Kerman (Southeast, Iran). Uric acid consuming bacteria was isolated by addition of poultry samples (1.0%) into enrichment medium (0.06% KH_2PO_4; 0.15% K_2HPO_4; 0.01% NaCl; 0.005% $CaCl_2$; 0.005% $MgSO_4$, $7H_2O$; 0.5% Uric acid; pH 7.5). These flasks were maintained in an orbital shaker incubator at 30 °C with shaking at 160 rpm for three days. After that, the culture was reassigned to the new medium three times. Then, samples were dispersed onto rich agar medium g/L (uric acid: 2.0; peptone: 4.0; NaCl: 1.0; beef extract: 2.0; agar: 20.0 and the pH was adjusted to 7.0). The initial screening was achieved by observing the presence of vibrant areas around the bacterial colonies representing zones of uric acid utilization (Ghosh and Sarkar, 2014). The strains forming larger areas at the same time were nominated for uricase production. Finally, the best isolates were also cultured on the specific agar medium (uric acid: 2.0; NaCl: 1.0; agar: 20.0 g/L), and the pH was adjusted to 7.0. GH3 isolate, which produced the highest halo around the colony at a shorter time, was selected as potent uricase-producing bacteria.

2.2. Identification of uricase-producing bacteria

The potent strain GH3 was recognized morphologically and biochemically agreeing with Bergey's Manual of Determinative Bacteriology (Ravikumar and Krishnakumar, 2010). Molecular identification of this isolate was performed by 16S rDNA gene sequencing, similar to previous reports (Ramezani-Pour et al., 2015; Azadian et al., 2016; Afrisham et al., 2016). The amplified 16S rDNA sequence of GH3 strain was recognized by relating their sequence to BLAST in NCBI. Multiple sequence alignment was performed by Clustal W, and phylogenetic analysis was also accomplished using the MEGA6 software (Tamura et al., 2007). A phylogenetic tree was also assembled by using the neighbor-joining manner (Saitou and Nei, 1987).

2.3. Uricase assay

The reaction of uricase activity contained 500 µl of uric acid (2 mM) dissolved in 100 mM sodium-borate buffer (pH 8.0), 100 µl of phenol (1.5%), 150 µl of 4-aminoantipyrine (25 mM), 50 µl of peroxidase (12 U ml^{-1}), and 100 µl of uricase solution. The reaction mixture was maintained at 30 °C for 30 min. The reaction was stopped by the adding of 1 ml of ethanol, and the absorbance was measured at 540 nm. One unit of uricase activity was defined as the quantity of enzyme that reliefs 1.0 µmol of H_2O_2 per min (Ravichandran et al., 2015).

2.4. Bacterial growth and uricase production

GH3 strain was added into 200 ml of medium, and the flask was maintained in an incubator for 72 h at 160 rpm at 30 °C. At diverse time intervals (12, 24, 36, 48, and 72 h) samples were picked up, and the cell biomass and uricase production (extracellular and intracellular) were measured. The fresh medium was also used as a blank. To investigate the time course of uricase construction, 25 µl of the cell free samples were poured to the wells of the uric acid specific agar plate. The clear halo was detected around the wells after 24 h of incubation (Ghosh and Sarkar, 2014).

2.5. Preparation of crude enzyme

GH3 strain was added into the 20 ml LB medium and maintained at 30 °C overnight to gain pre-culture as inoculum. The production medium (250 ml) was inoculated with 5% (v/v) inoculum and maintained at 30 °C, 170 rpm for 72 h. Bacterial cells were gathered by centrifugation with 10,000 rpm for 8 min at 4 °C, and then washed thrice with deionized water. Pellets were re-suspended in Na-phosphate buffer (0.5 M, pH 7.5) and were disturbed by sonication at 4 °C by protection sonifier output at 45 amplitude and giving 5 hits, each of 30 s, with 30 s break. The obtained homogenate was gathered at 12,000 rpm for 15 min at 4 °C. The resulting vibrant supernatant was gathered and used as crude uricase.

2.6. AgNPs synthesis and optimization

Three glass tubes, first containing 4 ml of cell extract of *Alcaligenes* GH3 with 2 mM $AgNO_3$, another having only cell extract, and the third having only $AgNO_3$ solution, were maintained for 24 h with 150 rpm. The presence of brown color from transparent was a pointer for the production of silver nanoparticles. Production of AgNPs was considered by using UV–vis spectral analysis during the process. In addition, biosynthesis of AgNPs was also investigated at different conditions such as temperatures (25, 35, 40 °C), pH (5.5, 7.0, 8.5), Ag^+ concentration (1, 2, 4 mM) and time (6, 12, 24, 48 h). Samples were picked up and AgNPs production was examined by using UV–vis spectral investigation, and detecting color intensity alterations throughout the process.

2.7. Characterization of AgNPs

2.7.1. UV–visible spectroscopy (UV–vis)

Change in the color change of reaction mixture was investigated through visual detection from pale yellow to brown. In addition, it was

completed by severe peaks detected by the absorption band of AgNPs by UV–vis spectrophotometer. At diverse time intervals, an aliquot of the sample was taken and examined for wavelength scanning from 300 to 700 nm (Singh et al., 2015).

2.7.2. Zeta potential analysis

Zeta potential quantities were achieved on a Malvern Zeta sizer at 25 °C with an occurrence wavelength at 633 nm and a 170° back sprinkle angle. The refractive index, viscosity, and absorption principles were delivered in the Malvern software for water (= 0.8872 cP, RI = 1.330). Nine runs were averaged for each fluid test for the purpose of precision.

2.7.3. Fourier transform infrared spectroscopy (FT-IR)

For FT-IR spectroscopy, AgNPs produced by cell extract of *Alcaligenes* GH3 strain was freeze-dried and subsequently diluted by KBr (the ratio 1:100). The FT-IR spectrum of the samples were observed on a JASCO FT-IR-4000 spectrophotometer device. All quantities were considered in the range from 400 to 4000 cm^{-1} at a resolution of 4 cm^{-1}. To recognize the functional groups present in the AgNPs samples, the spectral information was associated with the reference graph (Deepa et al., 2013).

2.7.4. Scanning electron microscopy

Scanning electron microscopy (SEM) was performed to detect the shape, morphology and size of the formed silver nanoparticles. A sample was done by object a drop of the blend onto an electric sanitary glass and permitting the solvent to vaporize. The training of scanning electron microscopy was examined on S-3400 2010 (Japan) at an increase speed voltage of 10,000 V (attached with a CCD camera) (Kumar et al., 2015).

2.8. Antibacterial evaluation of AgNPs

The antimicrobial activity of green formed AgNPs was considered alongside different bacterial pathogens. The bacterial test used were *P. aeruginosa*, *K. pneumoniae*, *E. coli*, *S. aureus*, *B. subtilis*, *S. typhimurium*, and *B. cereus*. The antibacterial activity of biologically formed silver nanoparticles was considered by well diffusion test (Priyaragini et al., 2013). The Mueller-Hinton agar plates were inoculated with 100 µl inoculum (1.5×10^8 CFU/mL) of each certain pathogen. Four wells were prepared with sterile borer into cultivated agar plates. The green formed AgNPs (70 µL) were discharged into one well of inoculated Mueller-Hinton agar plates. In the other two wells, an equal volume of $AgNO_3$ and cell extract was transferred. After incubation at 35 °C for 24 h, the region of inhibition was considered as average ± SD of the triplicate experiment.

2.8.1. Minimum inhibitory concentration

Minimum inhibitory concentration (MIC) of produced AgNPs against test pathogens (*E. coli*, *B. subtilis*, *P. aeruginosa*, *S. aureus* and *C. albicans*) was considered by well diffusion test on Mueller-Hinton agar (Perez et al., 1990; Bhatia et al., 2016). To observe the minimum inhibitory concentration of produced AgNPs, different concentrations of AgNPs were prepared. A uniform inoculum (1.5×10^8 CFU/mL) of each pathogen (100 µL) were picked up, and spread with sterile swabs. The wells with 8 mm size were prepared with sanitary borer into these agar plates. The lower slice of wells was wrapped with a petite molten agar. Subsequently, the different concentration of AgNPs were transferred into different wells of these cultivated plates. The obtained plates were maintained at 30 °C for 24 h. The lowest concentration of AgNPs that prevents the growth of pathogens was measured as the minimum inhibitory concentration (MIC).

2.8.2. Silver nanoparticles and their synergistic actions with antibiotics

The antimicrobial function of the produced silver nanoparticles was investigated against bacterial pathogens. The collective construction of AgNPs with standard antibiotic discs having a different manner of action contains: Ampicillin (AM, 10 µg/disc; beta-lactam antibiotics group), Ciprofloxacin (CIP, 5 µg/disc; fluoroquinolones group), Tetracycline (TE, 10 µg/disc; sulphonamides group), and Gentamicin (GN, 10 µg/disc; aminoglycoside). They were used to examine the synergistic effect of AgNPs-Ab against different bacterial pathogens. The plates were maintained at 30 °C for 24 h and the inhibition region (mm) was considered (Zarina and Nanda, 2014a,b). The rise in fold zone was valued by calculating the average clear inhibition region caused by an antibiotic alone and in blend with AgNPs (Fayaz et al., 2010; Zarina and Nanda, 2014a,b).

2.9. Antioxidant assays

The biosynthesized silver nanoparticles were investigated for antioxidant activity using three approaches as follows.

2.9.1. Scavenging of DPPH radicals

The efficiency of silver nanoparticles for scavenging DPPH (2, 2-diphenyl-1-picrylhydrazyl) radical was considered using the procedure of Chang and coworkers (Chang et al., 2002). Different concentration of silver nanoparticles (12.5, 25, 50, 100 and 200 µg/ml) were dispersed in methanol. To each sample, the equivalent volume of DPPH solution (0.135 mM in methanol) was added, vortexed thoroughly and left in the dark for 30 min at room temperature. The absorbance of the diverse samples was investigated at 517 nm. The capacity of silver nanoparticles to scavenge the DPPH radical was measured as a percentage of inhibition as follows:

$$Inhibition\ (\%) = \frac{ODcontrol - ODsample}{ODcontrol} \times 100$$

2.9.2. ABTS cation radical scavenging assay

The scavenging activities of $ABTS^+$ were measured as described by Mohan and coworkers with minor alterations (Mohan et al., 2012). At first, $ABTS^+$ was produced by a combination of ABTS solution (7 mM) and potassium persulfate solution (2.45 mM) at a ratio of 2:1 (v/v) after keeping for 16 h at 30 °C in the dark. The newly formed $ABTS^+$ solution was diluted with ethanol to an absorbance of 0.70 ± 0.04 at 734 nm. The reaction system enclosed 50 µL of silver nanoparticles at concentrations of 10, 25, 40, 50, 70, 100 and 120 µg/mL and a 400 µL prepared $ABTS^+$ dilution. The blend was kept at 25 °C in the dark for 10 min, and then, the absorbance of the mixture at 734 nm (A734) was measured (Wang et al., 2018). The $ABTS^+$ solution without any antioxidants was stated as 100%. The $ABTS^+$ radical scavenging assay was measured as revealed in the following Eq.:

$$Inhibition\ (\%) = \frac{OD\ control - OD\ sample}{ODcontrol} \times 100$$

2.9.3. Total antioxidant assay

The total antioxidant activity of silver nanoparticles was calculated following the technique defined by Prieto and coworkers (Prieto et al., 1999). An aliquot of 300 µl of each concentration prepared as defined above was added to 3 ml of reagent solution (28 mM sodium phosphate, 4 mM ammonium molybdate, and 0.6 M sulfuric acid), maintained at 95 °C for 90 min. After cooling the samples, the absorbance of the solutions was considered at 695 nm, and the antioxidant activities were measured as % following this equation (Gomaa, 2017):

$$Total\ antioxidant\ (\%) = \frac{OD\ control - OD\ sample}{ODcontrol} \times 100$$

2.9.4. Reducing power

Fe^{3+} reducing capacity of silver nanoparticles was investigated by

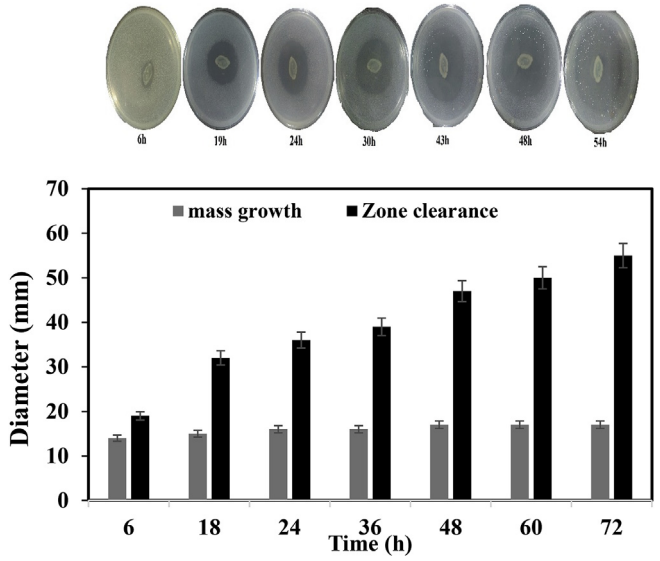

Fig. 1. a) Time course of cell growth and uric acid consumption of *Alcaligenes* GH3 on specific agar medium.

the manner of Oyaizu (1986). Different concentrations of silver nanoparticles (0.75 ml) were added with equivalent volumes of phosphate buffer (0.2 M, pH 6.6) and $K_3Fe(CN)_6$ (1%, w/v), maintained at 50 °C for 20 min. Trichloroacetic acid (TCA) solution (10%) was inoculated to stop the reaction and then centrifuged at 10,000 g for 15 min. Finally, $FeCl_3$ (0.1%, w/v) added to the diluted supernatant for 10 min, the absorbance was considered at 700 nm (Kida, 1966).

3. Results and discussion

3.1. Isolation and identification of the uric acid utilization strains

Four bacterial strains were isolated from poultry soil which could consume uric acid as a sole carbon and nitrogen sources. The development of the clearance zone around the colonies in specific agar plates directed utilization of uric acid. The most potent GH3 isolate which showed the highest area was designated for the following study. Fig. 1 showed the cell growth and uric acid consumption in specific agar media. Results showed that uricase production commenced after 6 h of incubation and reached the highest after 72 h of incubation (39 mm). Ghosh and Sarkar (2014) reported that uric acid was degraded by uricase from *Comamonas* sp. BTUA within 9 h and it reached 99% at 33 h of growth.

Genomic DNA of *Alcaligenes* GH3 was isolated, and the gene of 16S rDNA was amplified. The results of nucleotide BLAST defined scores of 16S rDNA sequence of GH3 isolated in association to analogous strains. GH3 isolate was categorized as genera *Alcaligenes*, having 97% maximum identity. Fig. 2 showed the phylogenetic relationships between *Alcaligenes* GH3 strain and some of the most strictly related species. Some recently identified bacteria for generating uricase have been reported as *Micrococcus*, *Brevibacterium,* and *Escherichia coli* (Kida, 1966), *Proteus vulgaris* (Azab, 2005), *Sphingobacterium thalpophilum* (Ravichandran et al., 2015), *Streptomyces albosriseolus* (Bongaerts and Vogels, 1976; Ammar et al., 1987), *Pseudomonas aeruginosa* (Khade et al., 2016), and *Bacillus thermocatenulatus* (Lotfy, 2008).

3.2. Synthesis of silver nanoparticles

Results showed that the GH3 strain produced about 42 U ml^{-1} after 48 h of cultivation. Formation of silver nanoparticles was confirmed by color alteration of the medium from pale yellow to dark brown (Fig. 3). Simultaneously, two other flasks, one contained only cell extract of *Alcaligenes* GH3, and the other contained only $AgNO_3$ solution were also used as controls. No color change of these two flasks established that cell extract of *Alcaligenes* GH3 with silver nitrate was owing to the construction of AgNPs (Fig. 3). The green synthesized AgNPs was characterized by UV–vis spectrum scanning (200–700 nm), as shown in Fig. 3. This technique investigates the absorption spectra of AgNPs production owing to collective excitation of conduction electrons in the Ag metal. So, it has been revealed to be an operational method for the nanoparticles analysis. It has been previously reported that the maximum absorbance of spherical AgNPs occurred between 420 and 450 nm (Talekar et al., 2014; Lateef et al., 2015a,b). Lateef et al. (2015a,b) showed that Keratinase from *Bacillus safensis* LAU13 produced AgNPs with dark brown color after 1.5 h of incubation.

3.3. Optimization of production of silver nanoparticles

Time course of silver nanoparticles synthesis by cell extract of *Alcaligenes* GH3 was also investigated by a color change and UV–Visible spectroscopy approaches. Results in Fig. 4, showed that biosynthesis of silver nanoparticles was perceived after 1 h of incubation and it reaches maximum after 24 h of incubation. It was noted that, no significantly AgNPs production was detected after 48 h of incubation. So, production after 24 h was used as the best time for NPs synthesis.

Results of the consequence of different pH values on the silver nanoparticles is shown in Fig. S1. These results indicate that the extreme of silver nanoparticles production was attained at pH 7.0, compared to other levels (pH 5.5, 8.0). At lower and higher pH, the absorbance and color change was respectively lower. It might be indicated that the reductase enzyme may be inactivated at the acidic and alkaline condition. Consequently, pH 7.0 was used as an optimized pH for the production of Ag nanoparticles and also it related to the surface charge and pI of the protein. Bio-synthesis of silver nanoparticles was also explored at diverse temperatures (25, 35, and 45 °C). As shown in Fig. S2, good production of silver nanoparticles was achieved at different studied temperatures. Although, the best fabrication of AgNPs was observed at 35 °C after 6 and 12 h of incubation, the synthesis of AgNPs were highest after 24 h of incubation at 35 and 45 °C. So, synthesis at 35 °C was selected for further studies. Effect of substrate concentration on the AgNPs production was investigated after 24 h of incubation. Cell extract was incubated with 1.0, 2.0, and 4.0 mM of $AgNO_3$. The highest production was observed at 4.0 mM, as shown in Fig. S3. But silver nanoparticles have been aggregated at this concentration. So, 2 mM of substrate concentration was used for further study. Patil et al. (2014) showed that the optimum conditions for the synthesis of silver nanoparticles were at pH 7.0, 0.05% of silver nitrate, 5 mg/ml of cells, and ambient temperature (26–36 °C).

3.4. Characterization of silver nanoparticles

The FTIR spectrum of Ag nanoparticles gives insight about the presence of different functional groups in the produced AgNPs to realize how bio-molecules like enzymes and proteins could probably perform as stabilizing, capping, and reducing agent for the biosynthesis of the Ag nanoparticles by the cell extract of uricase producing *Alcaligenes* GH3.

The FTIR spectrum analysis for silver nanoparticles signified deep absorption bands at 3447.20, 2920.95, 2851.78, 1634.48, 1543.03 and 1002.54 cm^{-1}, respectively, similar to previously reports (Zarina, and Nanda, 2014; Singh et al., 2016, 2018). The deep spectrum of FTIR peak at 3447 cm^{-1} was stated as the intense stretching vibrations of O–H functional group. In addition, this strong peak maybe related to the N–H stretch, which was specific of the amine group (Fig. 5A). Furthermore, the band at 2920 cm^{-1} point out C–H stretching of methylene groups of the protein. The moderate intense peak was detected at 1634 and 1543 cm^{-1} indicating C–O stretching of amides I, which is because of carbonyl stretch ambiances in the amide associations of

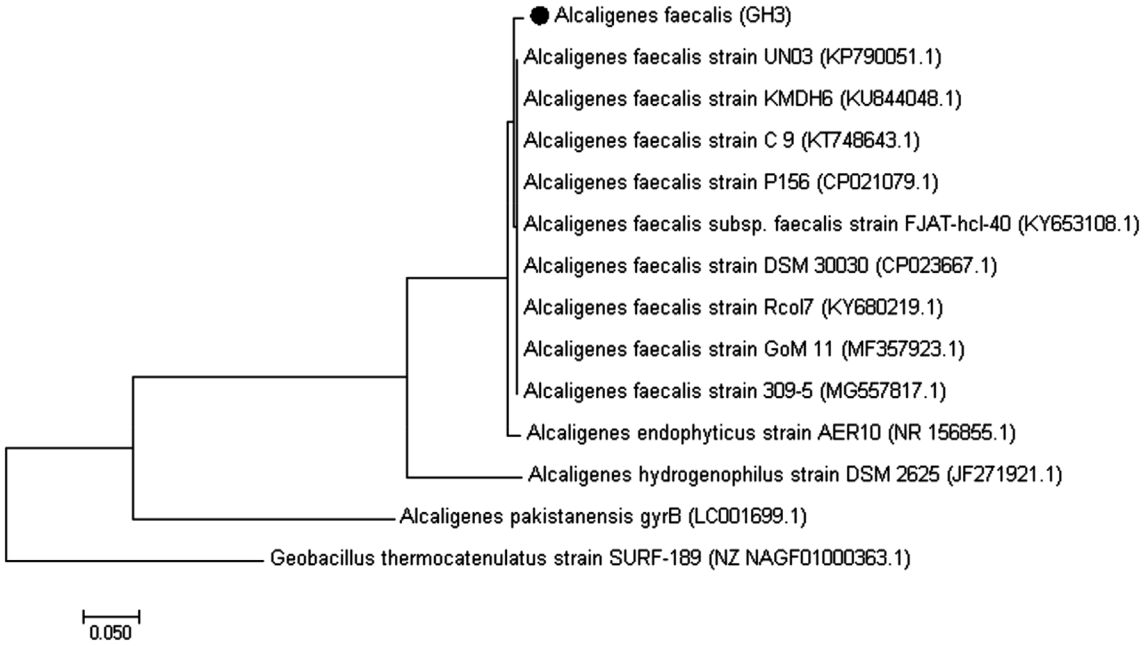

Fig. 2. Phylogenetic tree of GH3 strain showing relativeness with similar species. The branching pattern was generated by the neighbor-joining method (MEGA6 Genome sequencing software; based on 1000 replications, bootstrap percentages above 50% are shown).

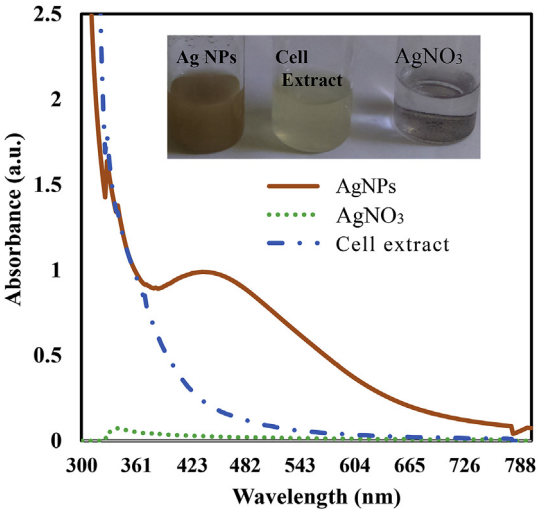

Fig. 3. UV Visible Spectrum analysis of biologically synthesized AgNPs.

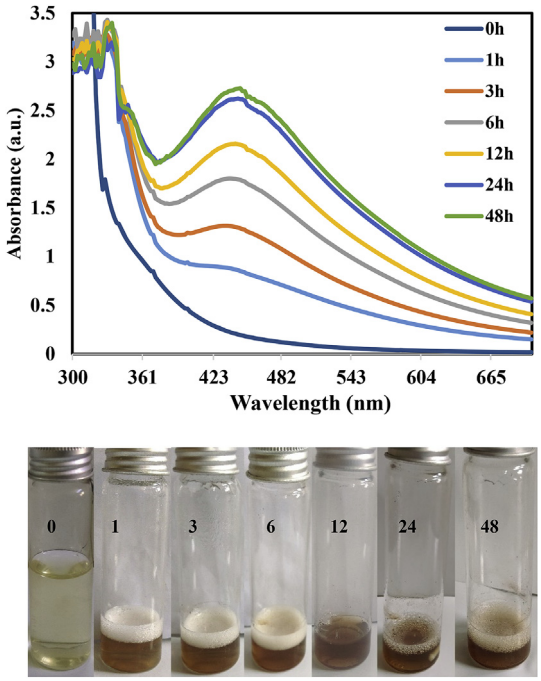

Fig. 4. Time course synthesis of AgNPs by cell extract of *Alcaligenes* GH3.

proteins (Ogi et al., 2010). Also, the typical peak 1002 cm^{-1} was attributed to the functional group of amide-II of proteins. These signs propose that the biomolecules existent in the cell extract of *Alcaligenes* GH3 could probably implement the function for the development of stable silver nanoparticles. It was identified that the silver nanoparticles could bind to protein through free amide groups, which designate that the proteins act as covering mediator for the stabilization of nanoparticles (Lok et al., 2006; Sarkar et al., 2007).

Results in Fig. 5B shown that AgNPs were globular in shape and were in size ranging from 32 to 49 nm. It specified that cell extract of *Alcaligenes* GH3 has a potent capacity for the biosynthesis of AgNPs. Devika and co-workers stated that the spherical AgNPs have a diameter that reached from 40 to 50 nm (Devika et al., 2012). Furthermore, Faghri and Salouti reported that the extracellular production of AgNPs was globular, and the size alternated from 10 to 100 nm (Faghri and Salouti, 2011). But, Bhosale and co-workers reported that the produced AgNPs were irregular in shape (Bhosale et al., 2015), while Saminathan presented that the average size of produced AgNPs was larger than 50 nm and globular in shape (Saminathan, 2015).

In the literature, α-amylase was used for AgNPs synthesis, which their shapes were hexagonal and triangular with sizes ranging from 22 to 44 nm (Mishra et al., 2012) while spherical AgNPs synthesized by laccase exhibited effective antimicrobial activities (Durán et al., 2014; Lateef et al., 2015a,b). In addition, keratinase synthesized spherical-shaped AgNPs of 5.0–30 nm with strong antibacterial activities (Lateef et al., 2015a,b). Also, nitrate reductase and cellulose have been used for synthesis of spherical-shaped AgNPs (Talekar et al., 2014). Furthermore, Lateef and Adeeyo produced AgNPs using Laccase of *Lentinus edodes* were walnut-shaped and the size ranged between 50 and 100 nm (Lateef and Adeeyo, 2015). Also, Azeez and co-workers showed that the

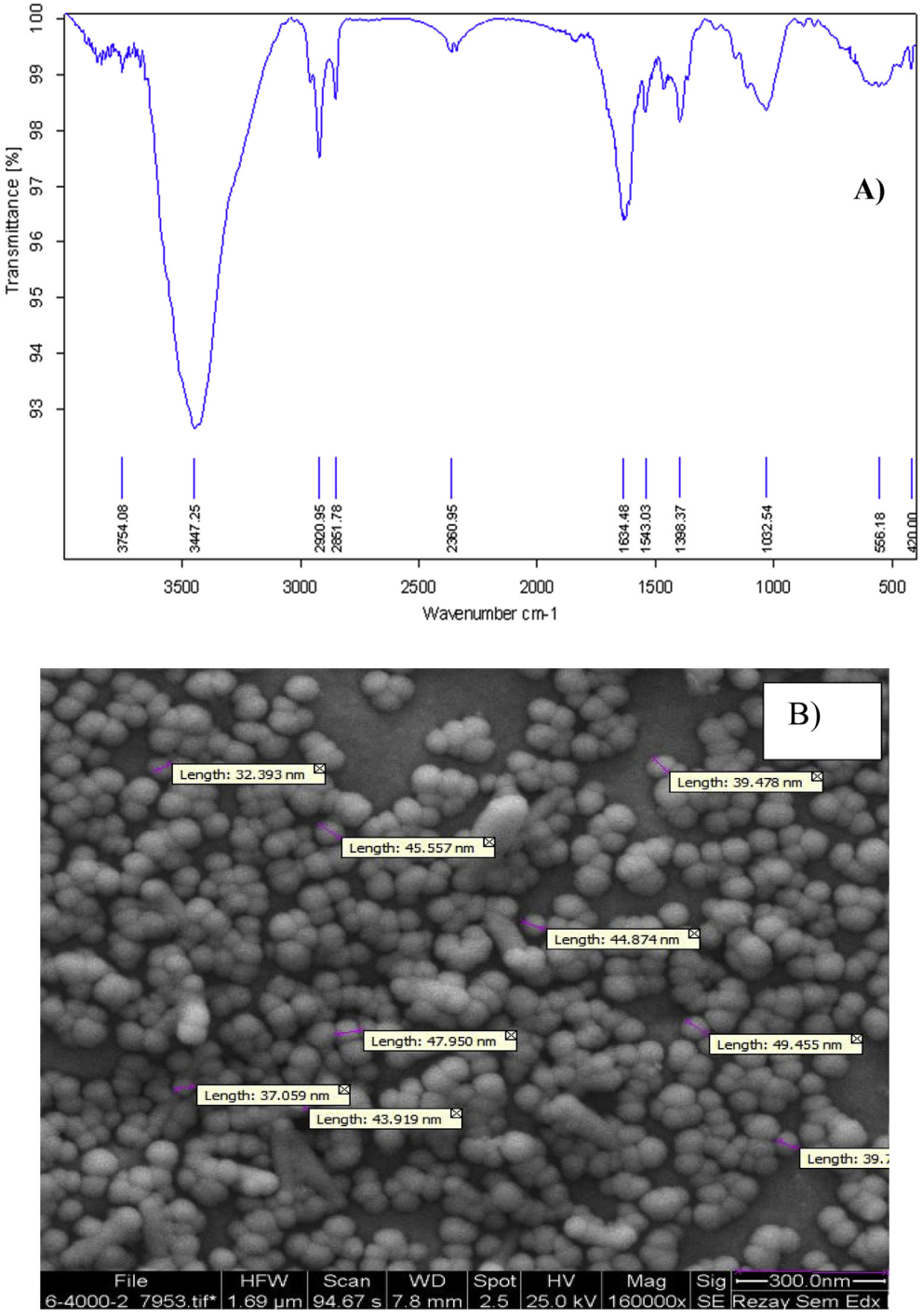

Fig. 5. FTIR and SEM analysis of biologically synthesized AgNPs.

spherical CBE-AgNPs had size variety of 8.96–54.22 nm (Azeez et al., 2017).

The DLS graph of green production of silver nanoparticles is revealed in Fig. 6A. The size stately by DLS technique is not only the size of AgNPs, but it also contains the compounds absorbed on the surface of metallic nanoparticles. Consequently, the size obtained by DLS method is higher than obtained by other methods. The zeta potential is a sign of the constancy of colloidal aqueous diffusions. Generally, particles with zeta potential (n > 30 mV) are assumed to be stabilized because of electrostatic revulsion (Jacobs and Muller, 2002). In this study, the zeta potential of synthesized silver nanoparticles in colloidal solution was −21 mV, which displays the outstanding stability of the silver nanoparticles in the colloidal solution (Fig. 6C).

3.5. Antibacterial activity of synthesized AgNPs

The antimicrobial activity of AgNPs explored against Gram-negative (*P. aeruginosa*, *K. pneumoniae*, and *E. coli*) and Gram-positive bacteria (*S. aureus*, *B. subtilis*, *S. typhimurium*, and *B. cereus*). AgNPs synthesized by cell extract of *Alcaligenes* GH3 displayed good antibacterial activity against all tested strains compared to control (Fig. S4). The Gram-negative bacteria (*E. coli*, *K. pneumoniae*) exhibited a maximum zone of inhibition of 13.10 mm, which might be because of the thicker cell wall of Gram positive bacteria compared to the Gram negative bacteria. So,

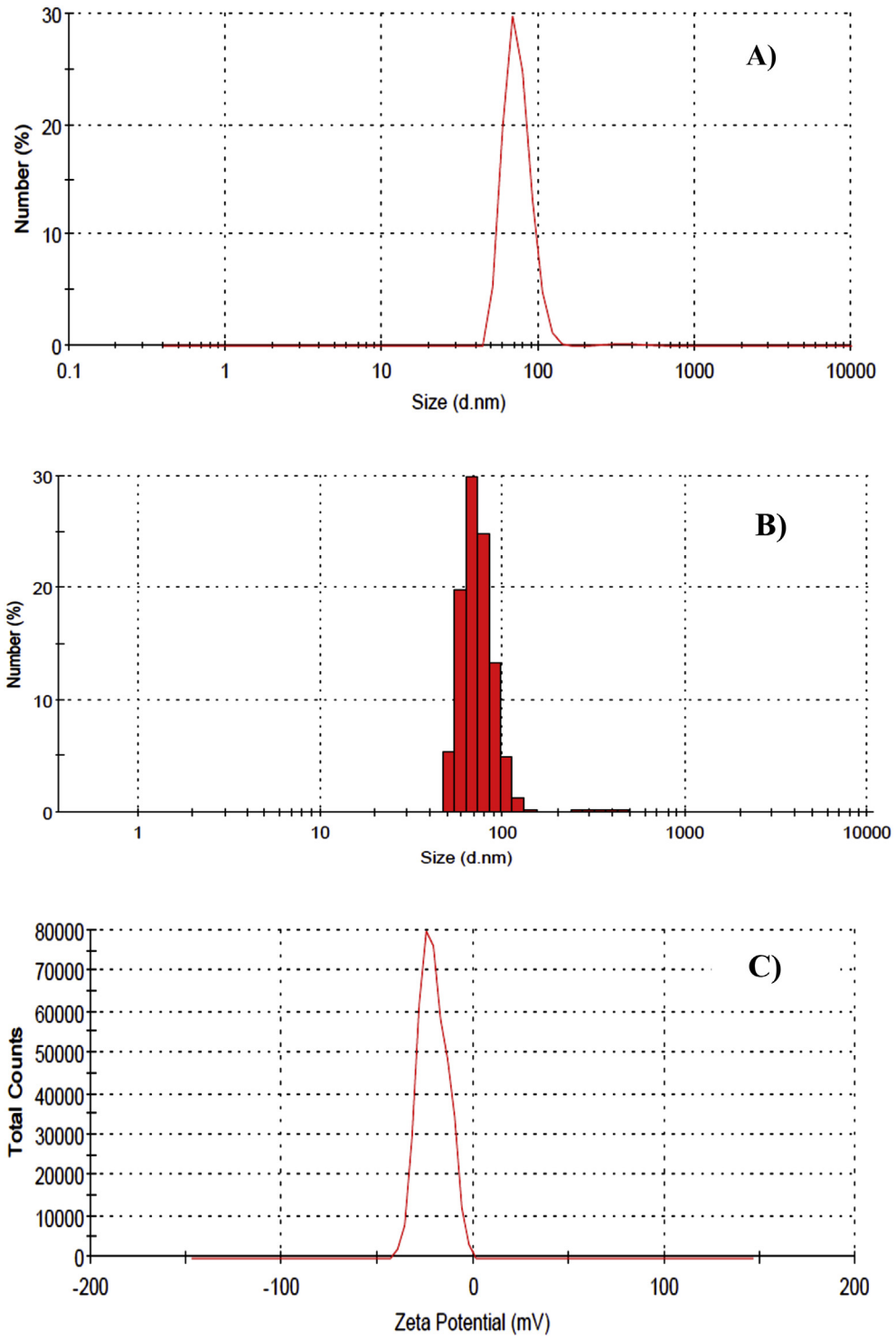

Fig. 6. DLS and Zeta potential analysis of biologically synthesized AgNPs.

this rigid structure causes difficult penetration of the AgNPs through the cell wall of Gram positive bacteria. Previously reports clarified that silver ions from AgNPs committed to the negatively charged bacterial cell wall and so, causes protein denaturation, gathering of envelope protein precursors, improved membrane permeability, the indulgence of the proton motive force, causing depletion of intracellular ATP and lastly cell death (Lin et al., 1998; Dibrov et al., 2002; Salopek-Sondi, 2004; Shrivastava, 2007; Anbu et al., 2019).

3.5.1. Determination of minimum inhibitory concentration

3.5.1.1. (MIC) of synthesized AgNPs. The zone of inhibition of diverse values of AgNPs around each well was studied and the average of three replicates presented in millimeter (Table 1). Results showed that the MIC against *S. aureus* and *B. cereus* was 15 µg/mL. Higher concentrations of silver nanoparticles (30 and 60 µg/mL, respectively) inhibited the growth of *P. aeruginosa* and *B. subtilis* (Table 1). Shrivastava and co-workers reported the MIC value of AgNPs against *S. aureus* as 100 µg/mol (Shrivastava et al., 2009), as well as in the report of Dos Santos et al. (2014). The MIC of silver nanoparticles

Table 1
MIC of silver nanoparticles by agar disc diffusion assay.

Zone of inhibition (mm)					
pathogen	Silver nanoparticles concentration (in μg/ml)				
	256	128	64	32	16
P. aeruginosa	8.5 ± 0.1	8 ± 0.3	7.5 ± 0.23	7 ± 0.1	0
S. aureus	9.5 ± 0.21	9 ± 0.2	8.5 ± 0.4	8 ± 0.1	7 ± 0.1
B. subtilis	10 ± 0.12	9 ± 0.1	8.5 ± 0.2	0	0
B. cereus	10.5 ± 0.11	10 ± 0.3	10 ± 0.2	9.5 ± 0.5	9 ± 0.13

against *P. aeruginosa* has been stated as 75 μg/mL, and 20 μg/mL in two dissimilar studies (Palanisamy et al., 2014). But the MIC of AgNPs against *B. subtilis* was reported as 40 μg/mL (Ruparelia et al., 2008).

Some parameters such as source and strain of pathogens, stabilization method in nanoparticles synthesis and diverse size and shape of nanoparticles are some factors that are responsible for the different values of MIC for the same pathogens (Pal et al., 2007). Furthermore, other factors include releasing of Ag from AgNPs, the value of the surface-to-volume ratio effect on the bactericidal activity of silver nanoparticles (Stobie et al., 2008). So, the silver nanoparticles produced using eco-friendly and green way can be used for biomedical application.

3.5.2. Synergistic effect of synthesized AgNPs with antibiotics

The different bacterial pathogens displayed diverse susceptibilities to silver nanoparticles. The mutual effect of silver nanoparticles with four standard antibiotic discs (Ampicillin, Tetracycline, Ciprofloxacin and Gentamicin) was considered against some pathogenic bacteria (*P. aeruginosa, K. pneumoniae, E. coli, K. planticola, S. aureus, B. subtilis, S. typhimurium,* and *B. cereus*). The inhibition area for standard antibiotics alone, and in blend with $AgNO_3$ and AgNPs established an important rise in the fold zone for the most pathogenic bacteria (Table 2).

Results showed that the maximum improvement in the antibacterial activity of AgNPs mixed with antibiotic were about 162.5 and 122.2% for ampicillin against *B. cereus* and tetracycline against *E. coli,* respectively, compared to antibiotic alone. In spite of that, the negative results also obtained for AgNPs-Ab complex, which yields lower area of inhibition when associated with the antibiotic area, such as Gentamicin against *K. planticola* and Ampicillin against *S. aureus*. Similar results were also reported that the combination of silver nanoparticles with antibiotics improved the antimicrobial activity of standard antibiotics (Zarina and Nanda, 2014a,b; Fayaz et al., 2010). Rajeshkumar reported that the highest inhibition zone was obtained in the combination of AgNPs with Gentamycin and Ampicillin against *B. subtilis,* and *K. planticola*, respectively (Rajeshkumar et al., 2016). Sarkar et al. also stated that for *S. aureus* (ML 422), and *E. coli* (ATCC 10536) AgNPs revealed more bactericidal competence compared to penicillin (Sarkar et al., 2007).

Oladipo and co-workers exhibited that the development of 13.6–71.4, 8.3–57.1 and 71.4–85.7% were found for ampicillin, ciprofloxacin, and cefuroxime respectively when used in mixture of AgNPs (Oladipo et al., 2017). Azeez and co-workers were also enhanced activities of ampicillin, cefuroxime, cefixime, and erythromycin by 42.9–100% in synergistic studies (Azeez et al., 2017). Enhancement of activities of augmentin, ofloxacin, and cefixime to the adjustment of 7.4–142.9% was reached in synergistic training (Lateef et al., 2015a,b).

Table 2
Synergistic effect of antibiotics with and without silver nanoparticles against different pathogenic bacteria.

	Inhibition Zone (mm)			Antibiotic	Pathogenic bacteria
Improvement (%) of AgNPs-Ab mix to Ab alone	Ab + AgNPs[c]	Ab + $AgNO_3$[b]	Ab[a]		
+36.3	30	23	22	Gentamicin	***P. aeruginosa***
+45.4	32	23	22	Ciprofloxacin	
+94.4	35	29	18	Tetracycline	
+25.0	10	10	8	Ampicillin	
- 35	13	20	20	Gentamicin	***K. pneumoniae***
+14.8	31	23	27	Ciprofloxacin	
+112.5	34	16	16	Tetracycline	
−5.3	36	41	38	Ampicillin	
+111.5	19	10	9	Gentamicin	***E. coli***
+62.5	26	17	16	Ciprofloxacin	
+122.2	20	12	8	Tetracycline	
+150	20	10	8	Ampicillin	
−38.5	8.0	12.5	13	Gentamicin	***K. planticola***
+13.3	34	32	30	Ciprofloxacin	
−21.4	11.0	10.5	14	Tetracycline	
−5.9	16	14	17	Ampicillin	
+26.1	29	23	23	Gentamicin	***S. aureus***
+56.5	36	24	23	Ciprofloxacin	
+46.1	38	27	26	Tetracycline	
−33.3	8.0	10	12	Ampicillin	
+116.7	26	21	12	Gentamicin	***B. subtilis***
+36.8	26	18	19	Ciprofloxacin	
+88.9	34	23	18	Tetracycline	
+180	14	8	5	Ampicillin	
+22.7	27	24	22	Gentamicin	***S. typhimurium***
+15.4	30	26	26	Ciprofloxacin	
+87.5	30	30	16	Tetracycline	
+13.3	34	31	30	Ampicillin	
+50	30	25	20	Gentamicin	***B. cereus***
+43.5	33	25	23	Ciprofloxacin	
+68	42	25	25	Tetracycline	
+162.5	21	19	8	Ampicillin	

[a] Ab = Antibiotic alone.
[b] Ab + $AgNO_3$ = Antibiotic with silver nitrate.
[c] Ab + AgNPs = Antibiotic with silver nanoparticles.

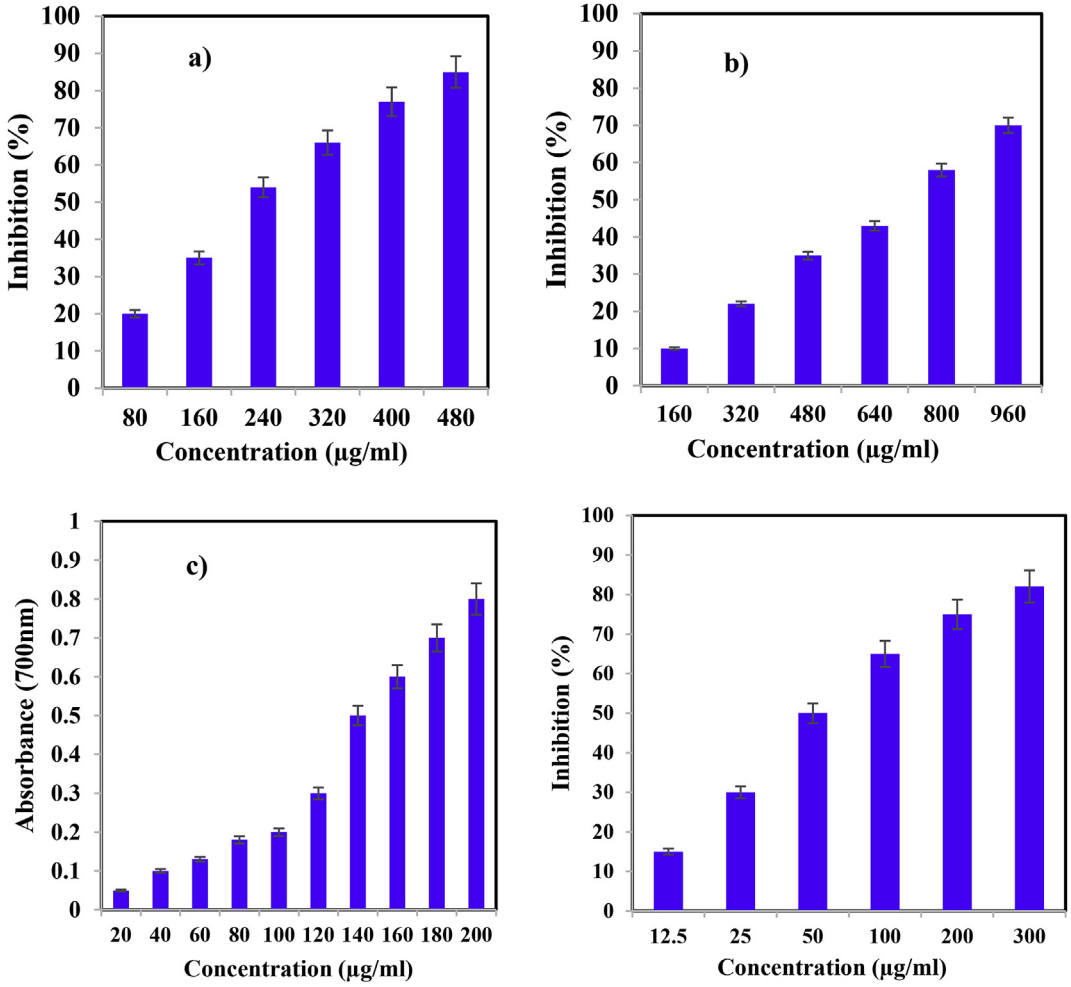

Fig. 7. Antioxidant activity of AgNPs (A) DPPH free radical scavenging activity, (B) ABTS radical scavenging activity, (C) total antioxidant capacity, and (D) Reducing capacity assessment.

Lateef and Adeeyo described that the AgNPs prompted a 20 mm inhibitory area at 141 µg/ml concentration for AgNPs (Lateef and Adeeyo, 2015). The interaction between AgNPs, and phosphorus of biomolecules of the bacterial cell can helps the entry of these particles into the bacterial cell, so resulting in cell-killing (Lateef and Adeeyo, 2015; Oladipo et al., 2017; Lateef et al., 2015).

AgNPs and ampicillin interact with each other through weak bonds such as van der Waals forces. Also, antibiotics have some active functional groups such as hydroxyl groups on their surface which can definitely react with silver nanoparticles by chelation (Fayaz et al., 2010). This complex acts on the bacterial cell wall and then leading to diffusion of silver nanoparticles into the cell (Fayaz et al., 2010). Furthermore, phosphorus-containing elements like DNA, and sulfur-containing proteins are possible to be the favored positions for AgNPs binding (Bragg and Rainnie, 1974; McDonnell and Russell, 1999; MubarakAli, 2011). Fayaz and co-workers reported that AgNPs-ampicillin complex inhibits DNA unwinding and ciprofloxacin-AgNPs complex operated on DNA gyrase as compared to antibiotic or AgNPs alone (Fayaz et al., 2010). However, green synthesis of AgNPs using cell extract of *Alcaligenes* GH3 can make nanoparticles more biocompatible and reduce the adverse effects of chemical agents.

3.6. Antioxidant activity

Reactive oxygen species (ROS) triggered the destruction of complex cellular molecules such as proteins, carbohydrates, DNA, and lipids. This can lead to development of several diseases like cancer, cardiovascular diseases, renal failure, liver diseases, and inflammatory problems. Antioxidants are agents that limit the toxic effects of these oxidant reactions. The antioxidant activity of silver nanoparticles was considered using four diverse colorimetric assays. DPPH assay is constant, simple and more viable assay. Fig. 7a showed the results of the DPPH radical scavenging function of silver nanoparticles. The absorbance at 517 nm diminished when the concentration of silver nanoparticles improved from 160 mg/ml to 960 mg/ml signifying proliferation in free radical scavenging function. The IC_{50} value of silver nanoparticles was 710 mg/ml. Similar dose-dependent DPPH activity was reported by AgNPs biosynthesized (Seralathan et al., 2014; Moteriya et al., 2017; Wang et al., 2018). ABTS cation radical scavenging function of AgNPs is shown in Fig. 7b. $ABTS^+$ radical scavenging function increased by growing the value of silver nanoparticles. The IC_{50} value of silver nanoparticles was 220 µg/ml. The concentration dependent $ABTS^+$ radical scavenging assay in plant-mediated silver nanoparticles have been previously reported (Patra et al., 2016; Moteriya and Chanda, 2017; Moteriya, and Chanda, 2018; Khoshnamvand et al., 2019; Wang et al., 2018). The phosphomolybdenum process of whole antioxidant ability test was based on the reduction of Mo (VI) to Mo (V) by the antioxidant complex and development of a green phosphate/Mo (V) complex. The IC_{50} value of silver nanoparticles was 65 µg/ml (Fig. 7c). The same results were also obtained by silver nanoparticles synthesized by *Allium cepa* extract (Gomaa, 2017). The reducing ability of silver nanoparticles is shown in Fig. 7d. Results indicated that reducing power improved by growing the value of silver nanoparticles. The increased absorbance at 700 nm

showed an increase in reductive capacity of silver nanoparticles. Results obtained were similar to previously described parallel results in *Cleistanthus collinus* extract and *Caesalpinia pulcherrima* stem metabolites synthesized silver nanoparticles (Kanipandian et al., 2014; Moteriya and Chanda, 2017).

4. Conclusion

This study exhibits the creation and characterization of Ag nanoparticles by cell extract of uricase producing *Alcaligenes* GH3. Protein in the cell extract was responsible for the bio-reduction, stabilization, and capping agent of silver ions. DLS consideration displayed the spreading of silver nanoparticles in range of 30–50 nm and zeta potential exhibited very respectable consistency in colloidal solution. Silver nanoparticles produced by cell extract of *Alcaligenes* GH3 displayed excellent antibacterial activity against some Gram positive and Gram-negative bacteria. Furthermore, AgNPs-antibiotic complex showed excellent synergic effect on the most of tested pathogenic bacteria. In addition, it showed appreciated antioxidant properties with increasing concentration. Taken together, this study showed that biologically synthesized silver nanoparticles have an excellent capacity of an antimicrobial and antioxidant agent.

Acknowledgment

The authors express their gratitude to the Research Council of the Shahid Bahonar University of Kerman, Kerman, Iran for financial support during this project.

Appendix A. Supplementary data

Supplementary data to this article can be found online at https://doi.org/10.1016/j.bcab.2019.101257.

References

Abd-Elnaby, H.M., Abo-Elala, G.M., Abdel-Raouf, U.M., Hamed, M.M., 2016. Antibacterial and anticancer activity of extracellular synthesized silver nanoparticles from marine *Streptomyces rochei* MHM13. Egypt. J. Aquatic Res. 42, 301–312.

Adelere, I.A., Lateef, A., 2016. A novel approach to the green synthesis of metallic nanoparticles: the use of agro-wastes, enzymes, and pigments. Nanotechnol. Rev. 5 (6), 567–587.

Afrisham, S., Badoei-Dalfard, A., Namaki-Shoushtari, A., Karami, Z., 2016. Characterization of a thermostable, $CaCl_2$-activated and raw-starch hydrolyzing alpha-amylase from *Bacillus licheniformis* AT70: production under solid state fermentation by utilizing agricultural wastes. J. Mol. Catal. B Enzym. 132, 98–106.

Ammar, M.S., Elwan, S.H., EL-Shahed, A.S., 1987. *Egypt,* Uricolytic *Streptomyces albogriseolus* from an Egyptian soil. 1. Taxonomy and uricase production and properties. J. Microbiol. 22 (2), 261–279.

Anbu, P., Gopinath, S.C.B., Yun, H.S., Lee, C.G., 2019. Temperature-dependent green biosynthesis and characterization of silver nanoparticles using balloon flower plants and their antibacterial potential. J. Mol. Struct. 1177, 302–309.

Azab, E.A., Mervat, M.A., Magda, F., 2005. Studies on uricase induction in certain bacteria. Egypt. J. Biol. 7, 44–54.

Azadian, F., Badoei-dalfard, A., Namaki-Shoushtari, A., Hassanshahian, M., 2016. Purification and biochemical properties of a thermostable, haloalkaline cellulase from *Bacillus licheniformis* AMF-07 and its application for hydrolysis of different cellulosic substrates to bioethanol production. Mol. Biol. Res. Commun. 5, 143–155.

Azeez, M.A., Lateef, A., Asafa, T.B., Yekeen, T.A., Akinboro, A., Oladipo, I.C., Gueguim-Kana, E.B., Beukes, L.S., 2017. Biomedical applications of cocoa bean extract-mediated silver nanoparticles as antimicrobial, larvicidal and anticoagulant agents. J. Clust. Sci. 28, 149–164.

Bhatia, D., Mittal, A., Malik, D.K., 2016. Antimicrobial activity of PVP coated silver nanoparticles synthesized by *Lysinibacillus* varians. 3 Biotech. 6, 196–204.

Bhosale, R.S., Hajare, K.Y., Mulay, B., Mujumdar, S., Kothawade, M., 2015. Biosynthesis, characterization and study of antimicrobial effect of silver nanoparticles by *Actinomycetes* spp. Int. J. Curr.Microbiol. Appl. Sci. 2, 144–151.

Bongaerts, G.P.A., Vogels, G.D., 1976. Uric acid degradation by *Bacillus fastidiosus* strains. J. Bacteriol. 125, 689–697.

Bragg, P.D., Rainnie, D.J., 1974. The effect of silver ions on the respiratory chain of *Escherichia coli*. Can. J. Microbiol. 20 (6), 883–889.

Chaby, G., Viseux, V., Poulain, J.F., De Cagny, B., Denoeux, J.P., Lok, C., 2005. Topical silver sulfadiazine induced acute renal failure. Ann. Dermatol. Venereol. 132, 891–893.

Chang, W., Sei, C.K., Soon, S.H., Bong, K.C., Hye, J.A., Min, Y.L., Sang, H.P., Soo, K.K., 2002. Antioxidant activity and free radical scavenging capacity between Korean medicinal plants and flavonoids by assay-guided comparison. Plant Sci. 163, 1161–1168.

Deepa, S., Kanimozhi, K., Panneerselvam, A., 2013. Antimicrobial activity of extracellularly synthesized silver nanoparticles from marine derived *actinomycetes*. Int. J. Curr. Microbiol. Appl. Sci. 2 (9), 223–230.

Devika, R., Elumalai, S., Manikandan, E., Eswaramoorthy, D., 2012. Biosynthesis of silver nanoparticles using the fungus *Pleurotus ostreatus* and their antimicrobial activity. Sci. Rep. 12, 1–5.

Dibrov, P., Dzioba, J., Gosink, K.K., Hase, C.C., 2002. Chemiosmotic mechanism of antimicrobial activity of Ag^+ in *Vibrio cholera* antimicrob. Agents Chemother. 46, 2668–2670.

Dos Santos, C.A., Seckler, M.M., Ingle, A.P., Gupta, I., Galdiero, S., Galdiero, M., Gade, A., Rai, M., 2014. Silver nanoparticles: therapeutical uses, toxicity and safety issues. J. Pharm. Sci. 103, 1931–1944.

Durán, N., Cuevas, R., Cordi, L., Rubilar, O., Diez, M.C., 2014. Biogenic Silver Nanoparticles Associated with Silver Chloride Nanoparticles (Ag@AgCl) Produced by Laccase from *Trametes versicolor*, vol 3. Springer Plus, pp. 645–652.

Elegbede, J.A., Lateef, A., Azeez, M.A., Asafa, T.B., Yekeen, T.A., Oladipo, I.C., Adebayo, E.A., Beukes, L.S., Gueguim-Kana, E.B., 2018a. Fungal xylanases-mediated synthesis of silver nanoparticles for catalytic and biomedical applications. IET Nanobiotechnol. 12 (6), 857–863.

Elegbede, J.A., Lateef, A., Azeez, M.A., Asafa, T.B., Yekeen, T.A., Oladipo, I.C., Aina, D.A., Beukes, L.S., Gueguim-Kana, E.B., 2018b. Biofabrication of gold nanoparticles using xylanases through valorization of corncob by *Aspergillus niger* and *Trichoderma longibrachiatum*: antimicrobial, antioxidant, anticoagulant and thrombolytic Activities. Waste Biomass Valorizat. 1–11 (in press).

Fariq, A., Khan, T., Yasmin, A., 2017. Microbial synthesis of nanoparticles and their potential applications in Biomedicine. J. Appl. Biomed. 15, 241–248.

Fayaz, A.M., Balaji, K., Girilal, M., Yadav, R., Kalaichelvan, P.T., Venketesan, R., 2010. Biogenic synthesis of silver nanoparticles and their synergistic effect with antibiotics: a study against gram positive and gram-negative bacteria. Nanomed. Nanotechnol. Biol. Med. 6, 103–109.

Ghiut, I.D., Cristea, C., Croitoru, J., Kostc, R., Wenkertd, I., Vyridese, A., Anayiotose, F., Munteanua, D., 2018. Characterization and antimicrobial activity of silver nanoparticles, biosynthesized using *Bacillus* species. Appl. Surf. Sci. 438, 66–73.

Gholami-Shabani, M., Shams-Ghahfarokhic, M., Gholami-Shabanid, Z., Akbarzadeh, A., Riazi, G., Ajdarif, S., Amanig, A., Razzaghi-Abyaneh, M., 2015. Enzymatic synthesis of gold nanoparticles using sulfite reductase purified from *Escherichia coli*: a green eco-friendly approach. Process Biochem. 50, 1076–1085.

Ghosh, T., Sarkar, P., 2014. Isolation of a novel uric-acid-degrading microbe *Comamonas* sp. BT UA and rapid biosensing of uric acid from extracted uricase enzyme. J. Biosci. 39, 805–819.

Gomaa, E.Z., 2017. Antimicrobial, antioxidant and antitumor activities of silver nanoparticles synthesized by *Allium cepa* extract: a green approach. J. Gen. Eng. Biotechnol. 15, 49–57.

Jacobs, C., Muller, R.H., 2002. Production and characterization of a budesonide nanosuspension for pulmonary administration. Pharm. Res. 19, 189–194.

Kalishwaralal, K., Deepak, V., Pandian, S.R.K., Kottaisamy, M., Mani, B., Kanth, S., Kartikeyan, B., Gurunathan, S., 2010. Biosynthesis of silver and gold nanoparticles using *Brevibacterium casei*. Colloids Surfaces B Biointerfaces 77, 257–262.

Kanipandian, N., Kannan, S., Ramesh, R., Subramanian, P., Thirumurugan, R., 2014. Characterization, antioxidant and cytotoxicity evaluation of green synthesized silver nanoparticles using *Cleistanthus collinus* extract as surface modifier. Mater. Res. Bull. 49, 494–502.

Khade, S., Srivastava, S.K., Tripathi, A.D., 2016. Production of clinically efficient uricase enzyme induced from different strains of *Pseudomonas aeruginosa* under submerged fermentations and their kinetic properties. Biocatal. Agricult. Biotechnol. 8, 139–145.

Khoshnamvand, M., Huo, C., Liu, J., 2019. Silver nanoparticles synthesized using *Allium ampeloprasum* L. leaf extract: characterization and performance in catalytic reduction of 4-nitrophenol and antioxidant activity. J. Mol. Struct. 1175, 90–96.

Kida, J., Kunihisa, M., 1966. Studies on bacterial uricase (I) isolation of uricase producing bacteria and some cultural conditions for production. J. Ferment. Technol. 44, 789–796.

Kumar, C.G., Mamidyala, S.K., 2011. Extracellular synthesis of silver nanoparticles using culture supernatant of *Pseudomonas aeruginosa*. Colloids Surfaces B Biointerfaces 84, 462–466.

Kumar, P.S., Balachandran, C., Duraipandiyan, V., Ramasamy, D., Ignacimuthu, S., Abdullah, D.N., 2015. Extracellular biosynthesis of silver nanoparticle using *Streptomyces* sp. 09 PBT 005 and its antibacterial and cytotoxic properties. Appl. Nanosci. 5, 169–180.

Lateef, A., Adeeyo, A.O., 2015. Green synthesis and antibacterial activities of silver nanoparticles using extracellular laccase of *Lentinus edodes*. Not. Sci. Biol. 7, 405–411.

Lateef, A., Adelere, I.A., Gueguim-Kana, E.B., 2015a. *Bacillus safensis* LAU 13: a new source of keratinase and its multi-functional biocatalytic applications. Biotechnol. Biotechnol. Equip. 29, 54–63.

Lateef, A., Adelere, I.A., Gueguim-Kana, E.B., Asafa, T.B., Beukes, L.S., 2015b. Green synthesis of silver nanoparticles using keratinase obtained from a strain of *Bacillus safensis* LAU 13. Int. Nano Lett. 5, 29–35.

Lateef, A., Ojo, S.A., Akinwale, A.S., Azeez, L., Gueguim-Kana, E.B., Beukes, L.S., 2016a. Biogenic synthesis of silver nanoparticles using cell-free extract of B*acillus safensis* LAU 13: antimicrobial, free radical scavenging and larvicidal activities. Biologia 70 (10), 1295–1306.

Lateef, A., Ojo, S.A., Oladejo, S.M., 2016b. Anti-candida, anti-coagulant and thrombolytic activities of biosynthesized silver nanoparticles using cell-free extract of *Bacillus safensis* LAU 13. Process Biochem. 51, 1406–1412.

Lin, Y.E., Vidic, R.D., Stout, J.E., McCartney, C.A., Yu, V.L., 1998. Inactivation of *Mycobacterium avium* by copper and silver ions. Water Res. 32, 1997–2000.
Lok, C.N., Ho, C.M., Chen, R., He, Q.Y., Yu, W.Y., Sun, H., Tam, P.K., Chiu, J.F., Che, C.M., 2006. Proteomic analysis of the mode of antibacterial action of silver nanoparticles. J. Proteome Res. 5 (4), 916–924.
Lotfy, W.A., 2008. Production of a thermostable uricase by a novel *Bacillus thermocatenulatus* strain. Bioresour. Technol. 99, 699–702.
McDonnell, G., Russell, A.D., 1999. Antiseptics and disinfectants: activity, action, and resistance. Clin. Microbiol. Rev. 12, 147–179.
Mishra, A., Sardar, M., 2012. Alpha-amylase mediated synthesis of silver nanoparticles. Sci. Adv. Mater. 4, 143–146.
Mohan, R., Birari, R., Karmase, A., Jagtap, S., Bhutani, K.K., 2012. Food Chem., Antioxidant activity of a new phenolic glycoside from *Lagenaria siceraria* stand. fruits. Food Chem. 132, 244–251.
Moteriya, P., Chanda, S., 2018. Biosynthesis of silver nanoparticles formation from *Caesalpinia pulcherrima* stem metabolites and their broad spectrum biological Activities. J. Gen. Eng. Biotechnol. 16, 105–113.
Moteriya, P., Padalia, H., Chanda, S., 2017. Characterization, synergistic antibacterial and free radical scavenging efficacy of silver nanoparticles synthesized using *Cassia roxburghii* leaf extract. J. Gen. Eng. Biotechnol. 15, 505–513.
MubarakAli, D., Thajuddin, N., Jeganathan, K., Gunasekaran, M., 2011. Plant extract mediated synthesis of silver and gold nanoparticles and its antibacterial activity against clinically isolated pathogens. Colloids Surfaces B Biointerfaces 85, 360–365.
Nakkala, J.R., Mata, R., Sadras, S.R., 2017. Green synthesized nano silver: synthesis, physicochemical profiling, antibacterial, anticancer activities and biological in vivo toxicity. J. Colloid Interface Sci. 499, 33–45.
Nanda, A., Nayak, B.K., Krishnamoorthy, M., 2018. Antimicrobial properties of biogenic silver nanoparticles synthesized from phylloplane fungus, *Aspergillus tamarii*. Biocatal. Agricult. Biotechnol. 16, 225–228.
Ocsoy, I., Tasdemir, D., Mazicioglu, S., Celik, C., Katı, A., Ulgen, F., 2018. Biomolecules incorporated metallic nanoparticles synthesis and their biomedical applications. Mater. Lett. 212, 45–50.
Ogi, T., Saitoh, N., Nomura, T., Konishi, Y., 2010. Room temperature synthesis of gold nanoparticles and nanoplates using *Shewanella* algae cell extract. J. Nanoparticle Res. 12, 2531–2539.
Oladipo, I.C., Lateef, A., Azeez, M.A., Asafa, T.B., Yekeen, T.A., Akinboro, A., Akinwale, A.S., Gueguim-kana, E.B., Beukes, L.S., 2017. Green synthesis and antimicrobial activities of silver nanoparticles using cell free-extracts of Enterococcus species. Not. Sci. Biol. 9 (2), 196–203.
Oyaizu, M., 1986. Studies on products of browning reaction—antioxidative activities of products of browning reaction. Prepared from glucosamine. Jpn. J. Soil Sci. Plant Nutr. 44, 307–315.
Pal, S., Tak, Y.K., Song, J.M., 2007. Does the antibacterial activity of silver nanoparticles depend on the shape of the nanoparticle; A study of the gram-negative bacterium *Escherichia coli*. Appl. Environ. Microbiol. 73, 1712–1720.
Palanisamy, N.K., Ferina, N., Amirulhusni, A.N., Zain, Z.M., Hussaini, J., Ping, L.J., Durairaj, R., 2014. Antibiofilm properties of chemically synthesized silver nanoparticles found against *Pseudomonas aeruginosa*. J. Nanobiotechnol. 12 (2), 1–7.
Patil, S., Fernandes, J., Tangasali, R., Furtado, I., 2014. Exploitation of *Haloferax alexandrinus* for biogenic synthesis of silver nanoparticles antagonistic to human and lower mammalian pathogens. J. Clust. Sci. 25, 423–433.
Patra, J.K., Das, G., Baek, K.H., 2016. Phyto-mediated biosynthesis of silver nanoparticles using the rind extract of watermelon (*Citrullus lanatus*) under photo-catalyzed condition and investigation of its antibacterial, anticandidal and antioxidant efficacy. J. Photochem. Photobiol. B Biol. 161, 200–210.
Perez, C., Paul, M., Bazerque, P., 1990. Antibiotic assay by agar well diffusion method. Acta biologia eet medicinae experimentalis 15, 113–115.
Premkumar, J., Sudhakar, T., Dhakal, A., Shrestha, J.B., Krishnakumar, S., Balashanmugam, P., 2018. Synthesis of silver nanoparticles (AgNPs) from cinnamon against BacterialPathogens. Biocatal. Agricult. Biotechnol. 15, 311–316.
Prieto, P., Pineda, M., Aguilar, M., 1999. Spectrophotometric quantitation of antioxidant capacity through the formation of a phosphomolybdenum complex: specific application to the determination of vitamin E. Aguilar. Anal. Biochem. 269, 337–341.
Priyadarshini, S., Gopinath, V., Priyadharsshini, N.M., MubarakAli, D., Velusamy, P., 2013. Synthesis of anisotropic silver nanoparticles using novel strain, *Bacillus flexus* and its biomedical application. Colloids Surfaces B Biointerfaces 102, 232–237.
Priyaragini, S., Sathishkumar, S.R., Bhaskararao, K.V., 2013. Biosynthesis of silver nanoparticles using *actinobacteria* and evaluating its antimicrobial and cytotoxicity activity. Int. J. Pharm. Pharm. Sci. 5 (2), 709–712.
Rajeshkumar, S., Malarkodi, C., Vanaja, M., Annadurai, G., 2016. Anticancer and enhanced antimicrobial activity of biosynthesizd silver nanoparticles against clinical pathogens. J. Mol. Struct. 1116, 165–173.
Ramezani-Pour, N., Badoei-Dalfard, A., Namaki-Shoushtari, A., Karami, Z., 2015. Nitrile-metabolizing potential of *Bacillus cereus* strain FA12; Nitrilase production, purification, and characterization. Biocatal. Biotransform. 33, 156–166.
Ravichandran, R., Hemaasri, S., Cameotra, S.S., Jayaprakash, N.S., 2015. Purification and characterization of an extracellular uricase from a new isolate of *Sphingobacterium thalpophilum* (VITPCB5). Protein Expr. Purif. 114, 136–142.
Ravikumar, S., Krishnakumar, S., 2010. Antagonistic activity of marine *actinomycetes* from Arabian Sea coast. Arch. Appl. Sci. Res. 2, 273–280.
Rostami, H., Khosravi, F., Mohseni, M., Rostami, A.A., 2018. Biosynthesis of Ag nanoparticles using isolated bacteria from contaminated sites and its application as an efficient catalyst for hydrazine electrooxidation. Int. J. Biol. Macromol. 107, 343–348.
Ruparelia, J.P., Chatterjee, A.K., Duttagupta, S.P., Mukherji, S., 2008. Strain specificity in antimicrobial activity of silver and copper nanoparticles. Acta Biomater. 4, 707–716.
Saitou, N., Nei, M., 1987. The neighbor-joining method: a new method for reconstructing phylogenetic trees. Mol. Biol. Evol. 4 (4), 406–425.
Salopek-Sondi, S.B., 2004. Silver nanoparticles as antimicrobial agent: a case study on *E. coli* as a model for Gram-negative bacteria. J. Colloid Interface Sci. 275, 177–182.
Saminathan, K., 2015. Biosynthesis of silver nanoparticles using soil *Actinomycetes Streptomyces* sp. Int. J. Curr.Microbiol. Appl. Sci. 4 (3), 1073–1083.
Sarkar, S., Jana, A.D., Samanta, S.K., Mostafa, G., 2007. Facile synthesis of silver nano particles with highly efficient anti-microbial property. Polyhedron 26, 4419–4426.
Seralathan, J., Stevenson, P., Subramaniam, S., Raghavan, R., Pemaiah, B., Sivasubramanian, A., Veerappan, A., 2014. Spectroscopy investigation on chemocatalytic, free radical scavenging and bactericidal properties of biogenic silver nanoparticles synthesized using *Salicornia brachiata* aqueous extract. Spectrochim. Acta A Mol. Biomol. Spectrosc. 118, 349–355.
Sharma, D., Kanchi, S., Bisetty, K., 2015. Biogenic synthesis of nanoparticles: a review. Arab. J. Chem. https://doi.org/10.1016/j.arabjc.2015.11.002.
Shivaji, S., Madhu, S., Singh, S., 2011. Extracellular synthesis of antibacterial silver nanoparticles using psychrophilic bacteria. Process Biochem. 46, 1800–1807.
Shrivastava, S., Bera, T., Roy, A., Singh, G., Ramachandrarao, P., Dash, D., 2007. Characterization of enhanced antibacterial effects of novel silver nanoparticles. Nanotechnology 18, 225103–225109.
Shrivastava, S., Bera, T., Singh, S.K., Singh, G., Ramachandrarao, P., Dash, D., 2009. Characterization of antiplatelet properties of silver nanoparticles. ACS Nano 3, 1357–1364.
Singh, H., Du, J., Singh, P., Yi, T.H., 2018. Extracellular synthesis of silver nanoparticles by *Pseudomonas* sp. THG-LS1.4 and their antimicrobial application. J. Pharmaceut. Anal. 8, 258–264.
Singh, P., Singh, H., Kima, Y.J., Mathiyalagan, R., Wang, C., Yang, D.C., 2016. Extracellular synthesis of silver and gold nanoparticles by *Sporosarcina koreensis* DC4 and their biological applications. J. Pharmaceut. Anal. 86, 75–83.
Singh, R., Shedbalkar, U.U., Wadhwani, S.A., Chopade, B.A., 2015. Bacteriagenic silver nanoparticles: synthesis, mechanism, and applications. Appl. Microbiol. Biotechnol. 99, 4579–4593.
Singh, R., Wagh, P., Wadhwani, S., Gaidhani, S., Kumbhar, A., Bellare, J., Chopade, B.A., 2013. Synthesis, optimization, and characterization of silver nanoparticles from *Acinetobacter calcoaceticus* and their enhanced antibacterial activity when combined with antibiotics. Int. J. Nanomed. 8, 4277–4290.
Sneha, K., Yun, Y.S., 2013. Recovery of microbially synthesized gold nanoparticles using sodium citrate and detergents. Chem. Eng. J. 214, 253–261.
Stobie, N., Duffy, B., McCormack, D.E., Colreavy, J., Hidalgo, M., McHale, P., Hinder, S.J., 2008. Prevention of *Staphylococcus epidermidis* biofilm formation using a low-temperature processed silver-doped phenyl triethoxysilane sol–gel coating. Biomaterials 29, 963–969.
Talekar, S., Joshi, G., Chougle, R., Nainegali, B., Desai, S., Joshi, A., Kambale, S., Kamat, P., Haripurkar, R., Jadhav, S., Nadar, S., 2014. Preparation of stable cross-linked enzyme aggregates (CLEAs) of NADH-dependent nitrate reductase and its use for silver nanoparticle synthesis from silver nitrate. Catal. Commun. 53, 62–66.
Tamura, K., Dudley, J., Nei, M., Kumar, S., 2007. MEGA4: molecular evolutionary genetics analysis (MEGA) software version 4.0. Mol. Biol. Evol. 24, 1596–1599.
Van der zande, M., Vandebrie, R.J., Van Doren, E., Kramer, E., Rivera, Z.H., Serrano-Rojero, C.S., Gremmer, E.R., Mast, J., Peters, R.J., Hollman, P.C., Hendriksen, P.J., Marvin, H.J., Peijnenburg, A.A., Bouwmeester, H., 2012. Distribution, elimination, and toxicity of silver nanoparticles and silver ions in rats after 28-day oral exposure. ACS Nano 6, 7427–7442.
Velmurugan, P., Iydroose, M., Hanif, M., Mohideen, A.K., Mohan, T.S., Cho, M., Oh, B.T., 2014. Biosynthesis of silver nanoparticles using *Bacillus subtilis* EWP-46 cell-free extract and evaluation of its antibacterial activity. Bioproc. Biosyst. Eng. 37 1527-1234.
Vijayabharathi, R., Sathya, A., Gopalakrishnan, S., 2018. Extracellular biosynthesis of silver nanoparticles using *Streptomyces griseoplanus* SAI-25 and its antifungal activity against *Macrophomina phaseolina*, the charcoal rot pathogen of sorghum. Biocatal. Agricult. Biotechnol. 14, 166–171.
Viswanathan, M., Arumugam, S., Thangavel, B., 2016. In vitro anticancer activity of silver nanoparticle synthesized by *Escherichia coli* VM1 isolated from marine sediments of Ennore southeast coast of India. Enzym. Microb. Technol. 95, 146–154.
Wadhwani, S.A., Shedbalkar, U.U., Singh, R., Chopad, B.A., 2018. Biosynthesis of gold and selenium nanoparticles by purified protein from *Acinetobacter* sp. SW 30. Enzym. Microb. Technol. 111, 81–86.
Wang, L., Wu, Y., Xie, J., Wu, S., Wu, Z., 2018. Characterization, antioxidant and antimicrobial activities of green synthesized silver nanoparticles from *Psidium guajava* L. leaf aqueous extracts. Mater. Sci. Eng. C 86, 1–8.
Wei, X., Luo, M., Li, W., Yang, L., Liang, X., Xu, L., Kong, P., Liu, H., 2012. Synthesis of silver nanoparticles by solar irradiation of cell-free *Bacillus amyloliquefaciens* extracts and $AgNO_3$. Bioresour. Technol. 103, 273–278.
Zarina, A., Nanda, A., 2014a. Combined efficacy of antibiotics and biosynthesised silver nanoparticles from *Streptomyces albaduncus*. Int. J. Pharm. Technol. 6 (6), 1862–1869.
Zarina, A., Nanda, A., 2014b. Green approach for synthesis of silver nanoparticles from marine *Streptomyces*- MS 26 and their antibiotic efficacy. J. Pharm. Sci. Res. 6 (10), 321–327.
Zonooz, N.F., Salouti, M., 2011. Extracellular biosynthesis of silver nanoparticles using cell filtrate of *Streptomyces* sp. ERI-3. Sci. Iran. F 18, 1631–1635.